EMMA BIGGS

Functional and anatomical connectivity in Complex Regional Pain Syndrome: A Multi-modal magnetic resonance imaging study

Original Paper

Pain processing relies on a distributed network of cortical regions. It is therefore proposed that cortical connectivity analyses may be useful for examining the abnormal cortical network interactions that modulate pain perception, and other symptoms, in chronic pain conditions. The present study used functional magnetic resonance imaging and diffusion weighted magnetic resonance imaging to investigate differences in functional and anatomical connectivity between healthy controls and patients with complex regional pain syndrome (type 1). It was hypothesised that this chronic pain condition would associate with changes in functional connectivity within resting-state networks, as well as changes in fractional anisotropy in white matter tracts. Results suggested that there is increased functional connectivity between regions of the sensorimotor resting-state network, and that there is decreased fractional anisotropy in the portion of the superior longitudinal fasciculus connecting these regions. These regions correspond to primary and secondary somatosensory cortices, which have been implicated in the sensory-discriminative aspect of pain processing. This supports the hypothesis that there are both functional and anatomical changes within pain processing networks, in patients with complex regional pain syndrome.
Keywords: chronic pain; connectivity; resting-state; fractional anisotropy

Emma E. Biggs; Master student Cognitive Neuroscience
Maastricht University, Maastricht, the Netherlands

e.biggs@student.maastrichtuniversity.nl

INTRODUCTION

Complex regional pain syndrome (CRPS) is a chronic pain disorder with a wide range of symptoms—that typically persist for over a year. There are two different types of CRPS: type I (CRPS-I; formerly known as reflex sympathetic dystrophy) which is preceded by mild tissue injury but no nerve damage, and type II (CRPS-II; formerly known as causalgia) which follows a nerve lesion (Patterson, Li, Smith, Smith, & Koman, 2011). In the Netherlands, incidence rates for CRPS are estimated to be 26.3 cases per 100,000 person-years (De Mos et al., 2007). The only identifiable risk factor appears to be limb immobilisation, and studies pre-CRPS show no differences in psychological state between those who do and do not develop CRPS (Marinus et al., 2011).

The main symptom of CRPS is spontaneous, diffuse pain, which covers an area larger than the area that suffered the initial trauma (De Boer et al., 2011). This pain is often described as a tearing or burning sensation (Patterson et al., 2011) that is not relieved by narcotics (Harke, Gretenkort, Ladleif, Rahman, & Harke, 2001), and spreads proximally as the disorder persists (Marinus et al., 2011). In addition to these symptoms, there are a wide range of physiological signs associated with CRPS; sensory signs include increased sensitivity to tactile stimulation (hyperesthesia) and to painful stimuli (hyperalgesia), as well as the perception of non-painful stimuli as extremely painful (allodynia). The affected limb may also display vasomotor (colour and temperature) changes, sudomotor signs (abnormal sweating), motor signs (decreased strength and slowness of movement) and oedema (swelling) (Maihöfner, Handwerker, & Birklein, 2006).

Changes in cognition and emotion have also been documented: studies have shown that patients mistakenly perceive sensations on their affected limb when tactile stimuli are applied to their unaffected limb (referred sensations; Maihöfner, Neundörfer, Birklein, & Handwerker, 2006). In addition, some patients report feeling that their affected limb does not belong to them (cognitive neglect; Swart, Stins, & Beek, 2009). In terms of emotional changes, patients often develop anxiety and a fear of the pain they experience as well as low mood or depression (Patterson et al., 2011).

The interaction between the peripheral nervous system, biochemical processes and implicated cortical networks produce these physiological, cognitive and emotional symptoms. For example, the trauma initiates an aberrant immune response (mediated by increased levels of cytokines) which leads to neurogenic inflammation, and this sensitises central and peripheral nervous systems (Alexander, Peterlin, Perreault, Grothusen, & Schwartzman, 2011; Kasper et al., 2005). These processes explain a number of the physiological symptoms seen in CRPS-I patients, such as: oedema, temperature changes, sudomotor changes, hyperesthesia, and hyperalgesia. Maladaptive neuroplasticity in white and grey matter may cause the other symptoms, such as allodynia, referred sensations, and anxiety.

In normal pain processing, the motor and somatosensory cortices are functionally connected with the posterior insular cortex—forming a sensory-discriminative network of pain processing. The affective-motivational network of pain processing includes the anterior insular cortex, the prefrontal cortex and

anterior cingulate cortex (Peltz et al., 2011). It should be noted that these regions are not specific to pain processing, but are thought to modulate the perception of pain as part of a wider network of areas that also show consistent activation during painful stimulation (Iannetti & Mouraux, 2010).

Research has shown that in CRPS-I patients, the density of the anterior insular cortex is decreased (Baliki, Schnitzer, Bauer, & Apkarian, 2011a) and its atrophy is negatively correlated to pain duration (Geha et al., 2009). The study by Geha et al. (2009) demonstrated that this applies to the right anterior insular cortex (which represents autonomic and visceral responses), irrespective of the sidedness of the affected limb. Furthermore, the right ventromedial pre-frontal cortex, which is crucial to emotional decision-making, has decreased grey matter density in patients with CRPS-I, and its decrease correlates negatively with pain duration and severity (Geha et al., 2009). These regions (the right anterior insular cortex and ventromedial pre-frontal cortex) are more connected in patients with CRPS-I, than in healthy controls (Geha et al., 2009), supporting the theory that there is altered affective-motivational pain processing in CRPS-I patients.

In addition to these structural changes, functional connectivity changes have also been documented in chronic pain patients. However, to the best of the author's knowledge, there is currently no research or scientific evidence that relates the changes in functional connectivity to CRPS-I. In chronic back pain patients the insular cortex has increased co-activation with the Default Mode Network (Buckner, Andrews-Hanna, & Schacter, 2008) (comprised of: orbital middle frontal gyrus, left and right angular gyri and precuneus), indicating abnormal interactions between resting-state networks (Tagliazucchi, Balenzuela, Fraiman, & Chialvo, 2010). Furthermore, chronic patients show more frequent temporal fluctuations in the insular cortex and anterior cingulate cortex compared to controls (Malinen et al., 2010), demonstrating the abnormal changes in both the spatial and temporal characteristics of resting state networks in patients suffering from chronic pain. These cortical changes worsen as the syndrome persists, and often return to normal following successful treatment (Schweinhardt & Bushnell, 2010).

The 'Connectivity' Approach

Previous research has already shown that neural activity can be indirectly captured using blood oxygen level dependent functional MRI (BOLD fMRI; Logothetis, Pauls, Augath, Trinath, & Oeltermann, 2001), and in a resting-state study this signal is obtained in the absence of stimuli. Participants are often asked to relax with their eyes open or closed, or passively view a fixation cross. The aim of resting-state data analyses is to extract, from the raw data, functional networks of cortical regions that co-activate in the absence of stimulation (e.g. the Default Mode Network, see Buckner et al., 2008). Different approaches to this extraction have been developed, and these can be classified into two categories: confirmatory and exploratory. In confirmatory analyses, (such as seed-based techniques) a region-of-interest (ROI, or time-course-of-interest) is already known and is used to find regions that show spatiotemporal synchronicity. These regions are subsequently interpreted as forming a functional network with the region-of-interest (Huettel, Song, & McCarthy, 2004). In exploratory analyses (such as independent component

analysis, ICA), the raw data is decomposed into a set of maximally independent components – spatial or temporal – where knowledge of one component provides no information about another (Hyvärinen & Oja, 2000). These components are then interpreted as forming a functional network. A benefit of this approach is that no prior regions-of-interest need to be included in the analysis, hence its suitability for exploratory analyses (Calhoun, Adali, Hansen, Larsen, & Pekar, 2003). As previous research fails to provide enough robust evidence to justify a confirmatory analysis approach, ICA appears best-suited to the present study.

It should be noted that functional connectivity maps cannot be used to infer direct anatomical connectivity, as often there is no direct anatomical connectivity between regions with strong functional connectivity (Honey et al., 2009). In order to investigate anatomical connectivity *in vivo*, diffusion-weighted MRI (DW-MRI) techniques must be employed. DW-MRI captures the self-diffusion (Brownian motion) of water molecules, exploiting the phenomenon that in white matter fibre bundles, water diffusion is anisotropic [i.e. follows one direction more easily than others (Conturo et al., 1999)]. The DW-MRI data are used to describe the movement of water molecules using a diffusion tensor (symmetric 3x3 matrix). This diffusion tensor also allows analyses such as fibre-tracking (Basser, Pajevic, Pierpaoli, Duda, & Aldroubi, 2000), or fractional anisotropy (FA). FA is a voxel-wise index describing "...the fraction of the tensor that can be assigned to anisotropic diffusion" (Jones, 2008, p.940), that is, the directionality of intravoxel diffusion. Values range from 1 (anisotropic: diffusion along one direction) to 0 (isotropic: diffusion direction is equal in all directions) and this value is often interpreted as an amalgamation of the microstructural properties of white matter, and intravoxel boundary orientation (Beaulieu, 2002; Chen, Blankstein, Diamant, & Davis, 2011; Mukherjee et al., 2008).

For the purposes of studying a chronic pain population, resting-state fMRI and DW-MRI have a number of benefits over traditional fMRI methods. First, as patients often feel pain in the absence of stimulation, an investigation of neural activity at rest can provide insights into key differences between patients and controls. Second, the processing of pain is thought to be distributed across a number of cortical regions and not localised to a specific region, therefore a connectivity approach may be more appropriate. Third, the combination of structural and functional connectivity allows the exploration of the relationship between functional and structural connectivity.

Research Questions and Hypotheses

The present study aims to investigate functional and anatomical connectivity in CRPS-I, using resting-state fMRI and DW-MRI, specifically focussing on changes in resting-state networks and fractional anisotropy. As of yet, this approach has not been used to study neuroplasticity in CRPS-I patients, and therefore we hope to elucidate: whether there are differences in connectivity between CRPS-I patients, and whether this novel methodology is an effective approach for studying chronic pain. This study will be divided into three research questions:

1. Are there differences in the spatio-temporal structure of r*esting-state* networks between CRPS-I patients and controls?

2. Are there differences in fractional anisotropy between CRPS-I patients and controls?
3. Are fractional anisotropy and resting-state functional connectivity related?

Findings from previous research have led to the designation of ventromedial prefrontal cortex, insular cortex, anterior cingulate cortex, nucleus accumbens, primary and secondary somatosensory cortex as regions-of-interest. Tracts-of-interest include the cingulum bundle and inferior fronto-occipital fasciculus.

METHOD

Participants

Six participants (three controls, three patients) took part in this study. The average age was 45.2 years, with a range from 24 to 61 years. Participant characteristics are summarised below (table 1). The data from 'study 1' and 'study 2' were collected in the context of two larger studies, and therefore there are some variations in data acquisition parameters, and procedure (see 'image acquisition' and 'procedure' for more details). Only details relevant to the present study are described.

Table 1. Participant characteristics.

Participant	Gender	Age	Handedness	Affected hand	Current pain rating
Control 1 (study 1)	Female	55	Right	n/a	n/a
Control 2 (study 1)	Female	24	Left	n/a	n/a
Control 3 (study 2)	Male	26	Right	n/a	n/a
Patient 1 (study 1)	Female	61	Ambidextrous	Left	5
Patient 2 (study 1)	Female	55	Right	Right	2
Patient 3 (study 1)	Male	31	Right	Right	7.5

Procedure

The present study required three MRI scans: resting-state fMRI, anatomical MRI, and diffusion-weighted MRI. In the scanner participants were in a supine position (head first), and instructed to remain as still as possible, there were no other visual or auditory cues. During the resting-state image acquisition participants were instructed to relax but remain awake with eyes closed (study 1), or keep their eyes open (study 2). Participants were provided with ear plugs, noise cancelling headphones with microphone and an emergency button. Before entering the scanner patients were asked to rate their current pain severity on a scale ranging

from 0 to 10 (0 = not at all, 10 = most pain ever felt).

Image Acquisition

MRI data were acquired using a 3.0 Tesla Siemens Allegra scanner at Maastricht University, with an 8-channel head coil. BOLD (blood oxygen level dependent) signal was recorded using a T2*-weighted gradient-echo echo planar imaging sequence. A total of 32 slices (voxel size of $3mm^3$, interleaved acquisition) were acquired [FOV = $216mm^2$, repetition time (TR), 2000ms; echo time (TE), 30ms; flip angle = 90°]. Diffusion-weighted images were obtained using a double re-focussed spin-echo EPI sequence (70 interleaved slices, voxel size of $2mm^3$, field-of-view $208mm^2$). Time-to-repeat (TR) was 8200ms, echo time (TE) 78ms and two b-values (0 s/mm^2 and 1000 s/mm^2) were organised into 36 non-collinear directions (twelve b=1000 s/mm^2 to every one b=0 s/mm^2). In study 1 a structural image was obtained using a T1-weighted sequence (ADNI-MPRAGE) with time-to-repeat (TR) 2250ms, time-to-echo (TE) 2.6ms and flip angle 9°. A total of 192 sagittal slices were obtained with a matrix size of $256mm^2$ and an in-plane-resolution of $1mm^3$. In study 2 the structural image was obtained using a GRAPPA 2 sequence with voxel size of $1mm^3$ (field-of-view $256mm^2$), time-to-repeat (TR) 2250ms, echo time (TE) 2.6ms and a flip angle of 9°.

Data Analysis

Resting-state fMRI

Data were analysed using BrainVoyager QX (Brain Innovation, Maastricht, the Netherlands; Goebel, Esposito, & Formisano, 2006). The anatomical image was pre-processed to correct inhomogeneities in intensity and transformed into Talairach space using rotation into the ACPC plane and a piecewise scaling transformation. The automatic segmentation tool was used to segment the grey and white matter, disconnect the hemispheres and remove bridges in the reconstruction of the cortex.

A 3D reconstructed mesh was created from the grey/white matter segmentation —this was manually corrected for errors— then smoothed using 50 iterations and simplified to 80,000 vertices. This process was carried out per hemisphere and per participant. These meshes were used as the basis for cortex-based curvature alignment (Frost & Goebel, 2012). This involved creating a smoothed curvature map and morphing into a sphere. In order to facilitate multi-subject alignment these spheres were mapped to a standard sphere with a reduced number of vertices. The standard spheres were used for group alignment to a dynamic group average.

The resting-state data were then pre-processed to correct for the interleaved acquisition of slices (slice scan-time correction by sinc interpolation) and motion correction (trilinear/sinc interpolation). These pre-processed images were then co-registered to their respective anatomical images and used to create a volume time-course, which was transformed into Talairach space (trilinear interpolation with a target resolution of 3x3x3mm). Temporal filtering of the time-courses was applied using a high-pass filter (5 cycles) and a Gaussian kernel (FWHM = 4s). Spatial smoothing consisted of a gaussian kernel (FWHM = 6mm).

To remove physiological noise and residual motion artifacts ROIs were defined in the ventricles and white matter (intensity masking). The time courses from these ROIs were used as predictors in a single-study general linear model (z-transformed); the residuals from this analysis were saved as a new, corrected, volume time course.

This corrected time course was then projected onto the 3D mesh created for cortex-based curvature alignment, sampling -1mm and +3mm from each vertex. This was then used as the basis for cortex-based fast ICA, following dimensionality reduction to 30 components (1/6 of the number of time-points) using principal component analysis (Formisano, Esposito, Di Salle, & Goebel, 2004). The resulting independent components were then aligned onto the 'group average' so all participants' data were curvature aligned. The independent components were then clustered using cortex-based self-organising group ICA (Esposito et al., 2005).

Using the clusters which were created during the self-organising group ICA, a second level analysis (random effects analysis of variance) was used to test for the main effect of a subset of group clusters (each group cluster individually), and between-group differences within individual clusters (α=0.05). This subset of clusters was selected by first qualitatively assessing the validity of the clustering of the independent components, and secondly excluding group clusters that were characterised by spatial patterns localised to the temporal or occipital lobes. The regions identified by this test were then used as seed-ROIs for fibre-tracking (discussed below: 'tractography'). Regions that spread over multiple gyri and sulci were reduced in size by increasing the significance threshold. The ROIs used as seed-ROIs for fibre-tracking were also used for further analyses of functional connectivity. Each individual's time course, for each ROI, was extracted and analysed in MatLab. Correlation coefficients were calculated between each ROI (within a group-independent component) and transformed into z-scores using Fisher's transformation. A t-test was used to investigate between-group differences in functional connectivity for each tract. Following this, tracts which showed a significant difference in functional connectivity between patients and controls, and also a significant difference in FA (see below) were subject to a correlation analysis to test whether the changes in FA were related to changes in functional connectivity.

Tractography & Fractional Anisotropy

ROIs were delineated on the cortex, using the results from the resting-state analysis. As the ROIs were identified from cortex-based aligned data, they were first transformed back into each individual participant's Talairach space, then to native space via ACPC. The ROIs were dilated (+1mm and -4mm from the selected vertex) so that they sufficiently overlapped with white matter.

The raw diffusion data was corrected for eddy-current distortion and motion in FSL (FMRIB, Oxford, United Kingdom; Smith et al., 2004; Woolrich et al., 2009) and then imported into BrainVoyager. Following this the diffusion image was co-registered to the anatomical image and voxels outside of the brain were masked. Sinc interpolation (R=3) to a target resolution of 2x2x2mm was used to create a diffusion-weighted volume. From this diffusion-weighted volume the diffusion tensors were calculated, these tensors were used for fibre tracking and for the creation of FA maps.

Deterministic fibre tracking, step-size 0.5mm, (using diffusion tensor calculations from FA analysis) identified tracks connecting ROIs within a group cluster (FA threshold = 0.2; projection threshold = 0.25; angle threshold = 50). The FA values of the voxels within each tract were extracted and analysed using histogram tables (20 bins: FA values ranging from 0-0.05, 0.05-0.1, 0.1-0.15, etc.) which were calculated for the extracted FA values of each tract and each participant. The number of voxels per FA 'bin' were converted into percentages, and then an average percentage per FA 'bin' for patients and controls was calculated. An ordinal chi-squared test on each tract tested for a linear-by-linear association between group (patient versus control) and FA value (the 20 'bins'). Tracts which showed a significant linear-by-linear association, following Bonferroni's correction for multiple comparisons, were further analysed by comparing mean FA values, for patients and controls, using t-tests.

Fractional Anisotropy

The raw diffusion-weighted data were corrected for eddy-current and motion distortions using affine registration to the first b=0 s/mm^2 image [FDT toolbox (Behrens et al., 2003)]. Voxels outside of the brain were masked, and a binary brain was created [BET toolbox (Smith, 2002)]. The diffusion tensor model was fitted to the images and used to create FA maps [FDT toolbox (Behrens et al., 2003)]. The images were then fed into the tract-based spatial statistics pipeline [TBSS (Smith et al., 2006)] which began with non-linear registration [FNIRT (Andersson, Jenkinson, & Smith, 2007a, 2007b)] to align the images to a standard image (FMRIB FA image) (Rueckert et al., 1999). An average was made of all participants' FA images, this was then thinned by removing voxels below the threshold FA value (threshold FA = 0.2) to create a mean FA skeleton, upon which each participants' FA data were projected. This 4D image was used as the input for permutation based t-test analyses (patients versus controls), and the extraction of mean FA values (per participant) for ROIs (regions from the JHU white matter tractography atlas, Mori, Wakana, & van Zijl, 2005). These mean FA values were compared with t-tests (patients versus controls).

RESULTS

Resting-state network analysis

An ANOVA was used to test the main effect for each group cluster (i.e. identify the resting-state network), and a contrast to compare the between-group differences within each group cluster (i.e. differences in spatial coherence between patients and controls, for that resting-state network). The contrasts revealed significant differences in component spatial structure for patients versus controls, in all four group clusters (t (145)>3, p=.0003, uncorrected for multiple comparisons, cluster-threshold = 50mm^2).

Group cluster one consists of a RSN, from all participants, that demonstrates co-activation in bilateral inferior parietal cortex and right middle frontal gyrus. A small number of regions in right parietal and frontal cortex show differential coherence

within this network, for patients versus controls. Group cluster two consists of a RSN, from all participants, that demonstrates co-activation in bilateral posterior cingulate cortex as well as a diffuse region overlapping the precuneus and parieto-occipital sulcus. For this network, patients and controls showed differing network coherence in a small region in the precuneus and posterior cingulate cortex. The third group cluster was characterised by diffuse ventral frontal (including ventral medial) cortex activation, with group differences in network coherence in the left superior frontal sulcus. The fourth group cluster consists of a RSN, from all participants, that demonstrates co-activation in right superior frontal gyrus and a diffuse region spreading across bilateral inferior pre- and post-central gyri and the central gyrus. On the right hemisphere this network also extends into the operculum. Differences in network coherence, for patients versus controls, appeared in the bilateral inferior central sulcus.

The functional connectivity was calculated between the ROIs that were also connected by tracts identified using fibre-tracking (table 2). T-tests showed a significant difference in functional connectivity, between patients (M=0.66, SD=0.07) and controls (M=0.48, SD=0.07), for tract 9, $t(4)$=-2.893, p=.04 (uncorrected for multiple comparisons). This tract was defined as part of the right superior longitudinal fasciculus [JHU white matter atlas, (Mori et al., 2005)], connecting right supramarginal gyrus and post-central gyrus.

Table 2. Regions-of-interest and tracts-of-interest for the four group clusters. The regions identified by the resting-state ANOVA analysis, which are connected by white matter tracts, are labelled as regions-of-interest. Centre-of-Gravity, size in standard deviation (SD), and size in number of voxels is also included. Coordinates given are in Talairach space.

Region-of-Interest		Centre-of-Gravity			Size (Standard Deviation)			Size (Voxels)
		x	y	z	x	y	z	
Cluster 1: ROI 1	Right Inferior Parietal Lobule	35.01	-56.88	40.87	8.49	9.75	5.65	9432
Cluster 1: ROI 2	Right Inferior Frontal Gyrus	44.25	1.09	22.09	3.18	3.5	3.12	935
Tract 1: ROI 1 & ROI 2	Right Superior Longitudinal Fasciculus							
Cluster 2: ROI 1	Right Cingulate Gyrus	3.42	-29.13	27.69	2.18	5.79	4.11	1673
Cluster 2: ROI 2	Right Cuneus	10.12	-66.61	29.19	5.75	6.74	8.08	9546
Cluster 2: ROI 3	Left Precuneus	-13.47	-66.15	26.1	5.37	6.98	9.68	10764
Tract 2: ROI 1 & ROI 2	Forceps Major							
Tract 3: ROI 1 & ROI 3	Forceps Major							
Tract 4: ROI 2 & ROI 3	Forceps Major							
Cluster 3: ROI 1	Right Subcallosal Gyrus	12.32	24.62	-7.87	7.00	13.43	4.4	9906
Cluster 3: ROI 2	Left Subcallosal Gyrus	-11.19	16.24	-9.53	6.40	14.7	4.27	8282
Cluster 3: ROI 3	Right Inferior Frontal Gyrus	40.36	36.19	2.42	6.17	6.89	5.55	4197
Tract 5: ROI 1 & ROI 2	Forceps Minor							
Tract 6: ROI 1 & ROI 3	Forceps Minor							
Cluster 4: ROI 1	Right Precentral Gyrus	47.76	-13.12	34.21	5.18	5.04	6.95	5043
Cluster 4: ROI 2	Left Precentral Gyrus	51.22	-15.02	27.24	5.18	8.16	11.74	6529
Cluster 4: ROI 3	Left Precentral Gyrus	-47.16	-10.9	33.24	5.79	5.48	7.21	5635
Cluster 4: ROI 4	Right Postcentral Gyrus	-52.83	-11.49	15.36	2.03	3.07	2.53	576
Cluster 4: ROI 5	Inferior Parietal Lobule	51.37	-37.36	31.58	3.16	3.12	4.71	1430
Tract 7: ROI 1 & ROI 2	Right Superior Longitudinal Fasciculus							
Tract 8: ROI 1 & ROI 5	Right Superior Longitudinal Fasciculus							
Tract 9: ROI 2 & ROI 5	Right Superior Longitudinal Fasciculus							
Tract 10: ROI 4 & ROI 3	Left Superior Longitudinal Fasciculus							

Tractography

Deterministic fibre-tracking identified a total of 10 tracts which connected ROIs within the components; these tracts were used as the basis for the comparison of FA values. The ordinal chi-square test revealed a significant linear-by-linear association between group and FA value for tract 1 (M^2=8.18, *df*=1, *p*=.04), tract 8 (M^2=41.55, *df*=1, *p*=.02), tract 9 (M^2=14.81, *df*=1, *p*<.001), and tract 10 (M^2=9.15, *df*=1, *p*<.001). Tracts 1, 8 and 9 are part of the right superior longitudinal fasciculus, whilst tract 10 is part of the left superior longitudinal fasciculus [JHU white matter atlas, (Mori et al., 2005)].

Tract 9 showed both a significant difference in functional connectivity, and FA values, for patients versus controls. A correlation analysis revealed a strong negative correlation between functional connectivity and FA in this tract, *r*=-0.90, *p*=.02 (figure 1).

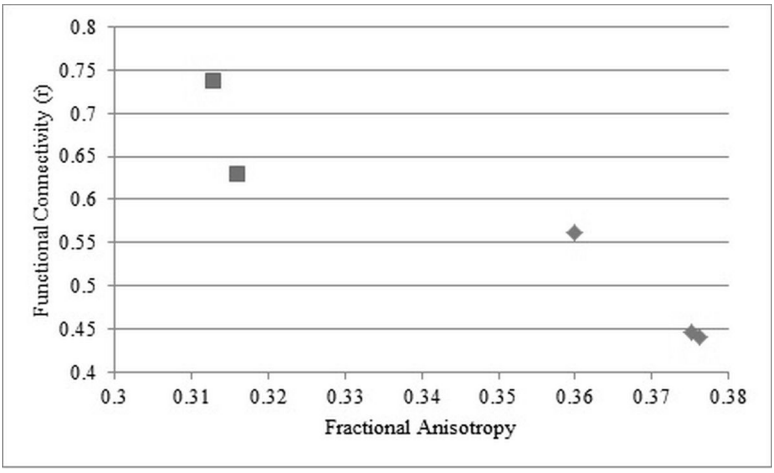

Figure 1: Graph showing functional connectivity as a function of fractional anisotropy, in tract 9, for each participant (Square = Patients; Diamond = Controls). There is a significant negative correlation between these measures (*r*=-0.90, *p*=.02). This tract is part of the right superior longitudinal fasciculus, and connects the right supramarginal gyrus and post-central gyrus.

Fractional Anisotropy

A voxel-wise t-test of the FA skeleton revealed no significant differences in FA values between patients and controls (α=.05). The mean FA values of the FA skeleton, left cingulum, right cingulum, and left inferior fronto-occipital fasciculus did not differ significantly different for patients versus controls. The difference between patients and controls for the right inferior fronto-occipital fasciculus was significant at *p*<.05 (see table 3).

Table 3. Comparison of fractional anisotropy values for CRPS-I patients compared to controls. **Significant difference between patients and controls (α=.05).*

Tract-of-interest	Patient	Controls	T-test
Mean FA skeleton	*M*=0.41, *SD*=0.01	*M*=0.43, *SD*=0.01	*t*(4)=2.66, *p*=.057
Left Cingulum	*M*=0.45, *SD*=0.02	*M*=0.47, *SD*=0.02	*t*(4)=2.02, *p*=.11
Right Cingulum	*M*=0.44, *SD*=0.03	*M*=0.46, *SD*=0.02	*t*(4)=1.28, p=.27
Left Inferior Fronto-occipital Fasciculus	*M*=0.42, *SD*=0.02	*M*=0.45, *SD*=0.01	*t*(4)=1.77, *p*=.15
Right Inferior Fronto-occipital Fasciculus	*M*=0.40, *SD*=0.01	*M*=0.43, *SD*=0.01	*t*(4)=3.68, *p*=.02*

DISCUSSION

The three research questions of this study focussed on: differences in spatiotemporal structure of resting-state networks; differences in white matter integrity; and whether these differences are related, for CRPS-I patients and controls. The results demonstrate that there are differences in functional and anatomical connectivity between CRPS-I patients and healthy controls. Specifically, resting-state networks show differential spatial structure, as well as increased functional connectivity between the right supramarginal gyrus and post-central gyrus, for CRPS-I patients compared to controls. Furthermore, portions of the right superior longitudinal fasciculus, which connected these regions, were found to have lower fractional anisotropy values for CRPS-I patients. Interestingly, the lower a participant's fractional anisotropy value, the higher their functional connectivity between these regions.

With regards to the differences in resting-state network spatiotemporal structure between controls and patients, the results support the hypotheses that resting-state networks show differential spatial structure and functional connectivity. Of particular functional relevance is the network referred to as 'group cluster 4', which appears to be consistent with a sensorimotor resting-state network (Biswal, Yetkin, Haughton, & Hyde, 1995; De Luca, Beckmann, De Stefano, Matthews, & Smith, 2006). The sensorimotor resting-state network is particularly relevant for CRPS-I, as the condition is characterised by a range of sensory and motor symptoms (e.g. hyperalgesia, bradykinesia). Within this network, the functional connectivity between the right supramarginal gyrus and post-central

gyrus was stronger for CRPS-I patients compared to controls. The post-central gyrus corresponds with the functional region of primary somatosensory cortex, whilst the region in the supramarginal gyrus appears to be consistent with the functional region of secondary somatosensory cortex (Eickhoff, Grefkes, Fink, & Zilles, 2008; Eickhoff, Amunts, Mohlberg, & Zilles, 2006). Both of these regions are also part of the sensory-discriminative network of pain processing (Peyron, Laurent, & García-Larrea, 2000).

This increased functional connectivity between right primary and secondary somatosensory cortex was ipsilateral to the affected limb for two patients and contralateral to the affected limb for one patient. As the data were not aligned by affected limb, nor were there enough patients to test the effect of the side of the affected limb, it is not possible to draw a robust conclusion from this result. Possible interpretations of this result are: (i) the altered functional connectivity is relates to the side of the affected limb (perhaps the result of compensatory behaviours), (ii) the altered functional connectivity is lateralised to the right hemisphere, irrespective of the side of the affected limb. This is similar to the result observed by Geha et al. (2009), that in CRPS-I patients there was a lateralised decrease in grey matter density of the right anterior insular cortex.

Concerning the anatomical connectivity, the white matter integrity of the superior longitudinal fasciculus (subdivision III), which connects the supramarginal gyrus with the ventral pre-motor and pre-frontal regions, differed significantly for CRPS-I patients compared to controls. Specifically, fractional anisotropy was lower for patients than controls in the left portion of the superior longitudinal fasciculus, and the distribution of values for both the right and left portions was different. These results strongly suggest that CRPS-I patients have altered white matter integrity in this—perhaps even a global decrease in white matter integrity. Consistent with this conclusion is the result that there is a trend for lower fractional anisotropy values in both bilateral cingulum and bilateral inferior fronto-occipital fasciculus, as well as a decrease in overall mean fractional anisotropy (p=.058). The pattern of lowered fractional anisotropy values is also consistent with the results from the study by Geha et al. (2009), where they found decreased fractional anisotropy in the left cingulum-callosal bundle.

Finally, the third research question was directed at the relationship between fractional anisotropy and functional connectivity. The functional connectivity of the third subdivision of the right superior longitudinal fasciculus correlated negatively with the FA values. If lower fractional anisotropy values indicate compromised white matter integrity, then an indirect white matter pathway may modulate the functional connectivity. However, if the decrease in fractional anisotropy is due to a factor which improves the propagation of action potentials, then this white matter tract may facilitate the functional connectivity in CRPS-I patients. Since it is not possible to conclude that lower fractional anisotropy values indicate damaged white matter, it is not possible to draw a concrete conclusion from this result (Jones, Knösche, & Turner, 2012).

The total number of participants limits the present study: with a larger sample the statistical power would increase and the analysis could take into account the large degree of intra-group variability. Patients with CRPS-I often suffer from

a wide range of symptoms, and as a result a dichotomous patient and control comparison may not be accurate. Pain duration and severity, which have previously been shown to exacerbate cortical changes, further confound the assumption that CRPS-I patients can be grouped as a homogenous population (Baliki, Schnitzer, Bauer, & Apkarian, 2011b; Chen et al., 2011; Geha et al., 2009). Therefore, a larger sample of participants would allow the introduction of a within-group variable of symptom, and also pain duration and/or severity. These changes would hopefully increase the sensitivity of the analyses to cortical changes associated with CRPS-I, specific symptoms, and the effect of pain duration and severity. Additionally, the matching of controls and patients could be improved in order to reduce the effect of demographic variability, and patients' data could be aligned by affected limb to avoid variability due to lateralisation of cortical changes.

With regards to image acquisition, participants in study one were instructed to keep their eyes closed during the resting-state scan. However, research has demonstrated that resting-state networks show significantly stronger correlations when participants are instructed to keep their eyes open and focussed on a fixation cross (Van Dijk et al., 2010). The (control) participant in study two was instructed to keep his eyes open during the resting-state scan, although no fixation cross was presented due to practical limitations. It is unlikely that the different instruction given to study one and study two participants would have a significant effect on the resting-state data, as the study by van Dijk et al. (2010) found no significant difference between eyes open and eyes closed, but if the present study was replicated then it would be advisable to change the instruction to passive fixation.

In the resting-state data analysis there was a conversion from a whole brain to cortex-based data set (Formisano et al., 2004). This step has two main benefits, which are: a) the subsequent cortex-based alignment for group analyses, and b) the limiting of ICA to grey matter voxels. This is especially useful for ICA as one of the key assumptions underlying most ICA approaches is that the components are mixed in a linear fashion. McKeown and Sejnowski (1998) assessed the validity of these assumptions and found that non-linear mixing models may be more appropriate than linear mixing models. On the other hand, if the data is restricted to grey matter voxels, then the assumption of linear mixing is still valid (McKeown & Sejnowski, 1998). Furthermore, cortex-based alignment has been shown to improve inter-subject alignment, especially in frontal regions and regions around the central sulcus—both of which were regions-of-interest in the present study (Frost & Goebel, 2012). However, there is a risk involved with summarising grey matter data onto the vertices of the cortex mesh: depending on the grey and white matter segmentation, the data represented on the vertex may be sampled too deep (into white matter) and therefore not only summarising grey matter voxels.

The group level resting-state data analysis used the self-organising ICA approach. One limitation of this approach is that when the individual independent components are clustered based on spatial similarity, then there are not (by definition) *large* between-group differences in resting-state network spatial structure. Whilst this does limit comparisons of the spatial structure of a network, this aspect of self-organising ICA does not affect the functional connectivity calculations. For the purposes of this study this benefit outweighed the limitation,

as the functional connectivity correlations are the quantification of the strength and directionality (i.e. negative or positive) of the connectivity between regions.

To investigate differences in anatomical connectivity, the present study used a deterministic fibre-tracking method, which does not give an indication of how reliable the tracking result is. Within each voxel there is a degree of error associated with the determined fibre orientation, a fact exploited by probabilistic fibre-tracking methods. These approaches incorporate the probability density function of fibre orientations within a voxel, resulting in a map which quantifies the degree of certainty associated with the tract (Jones, 2008). Whilst this is a clear advantage over the deterministic approach, probabilistic tracking can (usually) only be carried out from one seed-point and not a multi-voxel region-of-interest and therefore was not a feasible approach for this study.

Two approaches to comparing fractional anisotropy values were used in this study: the first used tracts-of-interest defined using a white matter atlas, the second using fibre-tracking from functionally defined regions-of-interest. Whilst the atlas approach has a number of benefits in terms of anatomically focussed research questions, the functional approach integrates both functional and anatomical data (Kanaan et al., 2006). Essentially, both approaches are attempting to ensure that when comparing two or more participants, the data is well aligned. In the skeleton and mask approach the data is structurally aligned, so in principle location *x* corresponds to the same structure in all participants. In the fibre-tracking approach the data is functionally aligned: that is, the white matter being compared connects the same functionally-relevant grey matter regions. The advantage of one approach over another is largely dependent on the research question being asked. For example, is there a specific location or structure of interest? If so, then the skeleton and mask approach will allow a structural alignment of data and a 'standardisation', so that there are an equal number of voxels per person, per tract (a benefit for a number of statistical analyses). If the researcher is interested in the white matter that connects to (e.g.) insular cortex, then the fibre-tracking approach may be more relevant. This captures individual differences in the white matter connected to a specific region, and therefore, may be more useful for gauging the interaction between white matter, and its connected grey matter. However, there are some inherent limitations with both approaches: in the skeleton and mask approach there is an assumption that the white matter of the participants is well aligned, whilst no alignment is needed in the fibre-tracking approach, there is an assumption that the regions-of-interest are similarly placed for each participant. In the present study the regions-of-interest were demarcated on a group-average curvature-aligned cortex mesh, and then aligned to the participant's native space, via a number of transformations. However, one of these transformations could have introduced a large degree of variability: the projection of the region-of-interest from the cortex mesh onto a whole-brain volume (i.e. from a vertex to grey matter, which can vary in thickness). A consistent approach was adopted for this (+1mm and -4mm); however, the accuracy of this projection may have varied from participant to participant. Differences in grey matter thickness, or slight variations in the transformation to native space, may have resulted in varying degrees of overlap with white matter and thus affected the fibre-tracking results.

The present study questions whether or not functional and anatomical connectivity differs between CRPS-I patients and controls, and whether these differences relate to each other. The results suggest that functional connectivity increases between primary and secondary somatosensory cortex (both of which are part of the sensorimotor resting-state network) for CRPS-I patients. Interestingly, the white matter connecting these regions showed significantly decreased fractional anisotropy, and this correlates negatively with the functional connectivity observed. Whilst this study had a number of methodological limitations which prevent the drawing of robust conclusions, it demonstrates the feasibility of applying this analysis pipeline to patients with chronic pain. A number of amendments have been suggested to improve this analytical approach, which could allow a more comprehensive and sensitive investigation of neuronal connectivity in chronic pain.

REFERENCES

Alexander, G. M., Peterlin, B. L., Perreault, M. J., Grothusen, J. R., & Schwartzman, R. J. (2011). Changes in Plasma Cytokines and Their Soluble Receptors in Complex Regional Pain Syndrome. *The journal of pain : official journal of the American Pain Society*, *13*(1), 10–20. doi:10.1016/j.jpain.2011.10.003

Andersson, J., Jenkinson, M., & Smith, S. (2007a). *Non-linear optimisation*. Retrieved from www.fmrib.ox.ac.uk/analysis/techrep

Andersson, J., Jenkinson, M., & Smith, S. (2007b). *Non-linear registration, aka spatial normalisation*. Retrieved from www.fmrib.ox.ac.uk/analysis/techrep

Baliki, M. N., Schnitzer, T. J., Bauer, W. R., & Apkarian, a. V. (2011a). Brain Morphological Signatures for Chronic Pain. (R. M. Luque, Ed.)*PLoS ONE*, *6*(10), e26010. doi:10.1371/journal.pone.0026010

Baliki, M. N., Schnitzer, T. J., Bauer, W. R., & Apkarian, a. V. (2011b). Brain Morphological Signatures for Chronic Pain. (R. M. Luque, Ed.)*PLoS ONE*, *6*(10), e26010. doi:10.1371/journal.pone.0026010

Basser, P. J., Pajevic, S., Pierpaoli, C., Duda, J., & Aldroubi, a. (2000). In vivo fiber tractography using DT-MRI data. *Magnetic resonance in medicine : official journal of the Society of Magnetic Resonance in Medicine / Society of Magnetic Resonance in Medicine*, *44*(4), 625–32. Retrieved from http://www.ncbi.nlm.nih.gov/pubmed/11025519

Beaulieu, C. (2002). The basis of anisotropic water diffusion in the nervous system - a technical review. *NMR in biomedicine*, *15*(7-8), 435–55. doi:10.1002/nbm.782

Behrens, T., Woolrich, M., Jenkinson, M., Johansen-Berg, H., Nunes, R., Clare, S., Matthews, P., et al. (2003). Characterization and propagation of uncertainty in diffusion-weighted MR imaging. *Magnetic resonance in medicine*, *50*(5), 1077–1088.

Biswal, B., Yetkin, F. Z., Haughton, V. M., & Hyde, J. S. (1995). Functional Connectivity in the Motor Cortex of Resting Human Brain Using Echo-Planar MRI. *Magnetic resonance in medicine*, *34*, 537–541.

Buckner, R. L., Andrews-Hanna, J. R., & Schacter, D. L. (2008). The brain's default network: anatomy, function, and relevance to disease. *Annals of the New York Academy of Sciences*, *1124*, 1–38. doi:10.1196/annals.1440.011

Calhoun, V. D., Adali, T., Hansen, L. K., Larsen, J., & Pekar, J. J. (2003). ICA of functional MRI data: An overview. *Framework*, 281–288.

Chen, J. Y., Blankstein, U., Diamant, N. E., & Davis, K. D. (2011). White matter abnormalities in irritable bowel syndrome and relation to individual factors. *Brain research*, *1392*, 121–131.

doi:10.1016/j.brainres.2011.03.069

Conturo, T. E., Lori, N. F., Cull, T. S., Akbudak, E., Snyder, A. Z., Shimony, J. S., McKinstry, R. C., et al. (1999). Tracking neuronal fiber pathways in the living human brain. *Proceedings of the National Academy of Sciences of the United States of America*, *96*(August), 10422–10427.

De Boer, R. D. H., Marinus, J., Van Hilten, J. J., Huygen, F. J., Van Eijs, F., Van Kleef, M., Bauer, M. C. R., et al. (2011). Distribution of signs and symptoms of Complex Regional Pain Syndrome type I in patients meeting the diagnostic criteria of the International Association for the Study of Pain. *European journal of pain*, *15*(8), 830.e1–830.e8. doi:10.1016/j.ejpain.2011.01.012

De Luca, M., Beckmann, C. F., De Stefano, N., Matthews, P. M., & Smith, S. M. (2006). fMRI resting state networks define distinct modes of long-distance interactions in the human brain. *NeuroImage*, *29*(4), 1359–67. doi:10.1016/j.neuroimage.2005.08.035

De Mos, M., De Bruijn, G. J., Huygen, F. J. P. M., Dieleman, J. P., Stricker, B. H. C., & Sturkenboom, M. C. J. M. (2007). The incidence of complex regional pain syndrome: a population-based study. *Pain*, *129*(1-2), 12–20. doi:10.1016/j.pain.2006.09.008

Eickhoff, S B, Grefkes, C., Fink, G. R., & Zilles, K. (2008). Functional lateralization of face, hand, and trunk representation in anatomically defined human somatosensory areas. *Cerebral cortex (New York, N.Y. : 1991)*, *18*(12), 2820–30. doi:10.1093/cercor/bhn039

Eickhoff, Simon B, Amunts, K., Mohlberg, H., & Zilles, K. (2006). The human parietal operculum. II. Stereotaxic maps and correlation with functional imaging results. *Cerebral cortex (New York, N.Y. : 1991)*, *16*(2), 268–79. doi:10.1093/cercor/bhi106

Esposito, F., Scarabino, T., Hyvarinen, A., Himberg, J., Formisano, E., Comani, S., Tedeschi, G., et al. (2005). Independent component analysis of fMRI group studies by self-organizing clustering. *NeuroImage*, *25*(1), 193–205. doi:10.1016/j.neuroimage.2004.10.042

Formisano, E., Esposito, F., Di Salle, F., & Goebel, R. (2004). Cortex-based independent component analysis of fMRI time series. *Magnetic resonance imaging*, *22*(10), 1493–504. doi:10.1016/j.mri.2004.10.020

Frost, M. a, & Goebel, R. (2012). Measuring structural-functional correspondence: spatial variability of specialised brain regions after macro-anatomical alignment. *NeuroImage*, *59*(2), 1369–81. doi:10.1016/j.neuroimage.2011.08.035

Geha, P. Y., Baliki, M. N., Harden, R. N., Bauer, W. R., Todd, B., & Apkarian, A. V. (2009). The brain in chronic CRPS pain: Abnormal gray-white matter interactions in emotional and autonomic regions. *Neuron*, *60*(4), 570–581. doi:10.1016/j.neuron.2008.08.022.The

Goebel, R., Esposito, F., & Formisano, E. (2006). Analysis of functional image analysis contest (FIAC) data with Brainvoyager QX: From single-subject to cortically aligned group general linear model analysis and self-organizing group independent component analysis. *Human Brain Mapping*, *27*, 392–401.

Harke, H., Gretenkort, P., Ladleif, H. U., Rahman, S., & Harke, O. (2001). The response of neuropathic pain and pain in complex regional pain syndrome I to carbamazepine and sustained-release morphine in patients pretreated with spinal cord stimulation: A double-blinded randomised study. *Pain*, (9), 488–495.

Honey, C. J., Sporns, O., Cammoun, L., Gigandet, X., Thiran, J. P., Meuli, R., & Hagmann, P. (2009). Predicting human resting-state functional connectivity from structural connectivity. *Proceedings of the National Academy of Sciences of the United States of America*, *106*(6), 2035–40. doi:10.1073/pnas.0811168106

Huettel, S. A., Song, A. W., & McCarthy, G. (2004). *Functional Magnetic Resonance Imaging*. *Magnetic Resonance Imaging* (1st Editio.). Sunderland, MA: Sinauer Associates.

Hyvärinen, a, & Oja, E. (2000). Independent component analysis: algorithms and applications. *Neural networks : the official journal of the International Neural Network Society*, *13*(4-5), 411–30. Retrieved from http://www.ncbi.nlm.nih.gov/pubmed/10946390

Iannetti, G. D., & Mouraux, A. (2010). From the neuromatrix to the pain matrix (and back).

Experimental brain research, *205*(1), 1–12. doi:10.1007/s00221-010-2340-1
Jones, D. K. (2008). Studying connections in the living human brain with diffusion MRI. *Cortex; a journal devoted to the study of the nervous system and behavior*, *44*(8), 936–52. doi:10.1016/j.cortex.2008.05.002
Jones, D. K., Knösche, T. R., & Turner, R. (2012). White Matter Integrity, Fiber Count, and Other Fallacies: The Do's and Don'ts of Diffusion MRI. *NeuroImage*, 1–16. doi:10.1016/j.neuroimage.2012.06.081
Kanaan, R. a, Shergill, S. S., Barker, G. J., Catani, M., Ng, V. W., Howard, R., McGuire, P. K., et al. (2006). Tract-specific anisotropy measurements in diffusion tensor imaging. *Psychiatry research*, *146*(1), 73–82. doi:10.1016/j.pscychresns.2005.11.002
Kasper, D. L., Braunwald, E., Fauci, A. S., Hauser, S. L., Longo, D. L., & Jameson, J. L. (2005). *Harrison's Principles of Internal Medicine* (16th ed., p. 1907). McGraw-Hill.
Logothetis, N. K., Pauls, J., Augath, M., Trinath, T., & Oeltermann, a. (2001). Neurophysiological investigation of the basis of the fMRI signal. *Nature*, *412*(6843), 150–7. doi:10.1038/35084005
Maihöfner, C., Handwerker, H. O., & Birklein, F. (2006). Functional imaging of allodynia in complex regional pain syndrome. *Neurology*, *66*(5), 711–7. doi:10.1212/01.wnl.0000200961.49114.39
Maihöfner, C., Neundörfer, B., Birklein, F., & Handwerker, H. O. (2006). Mislocalization of tactile stimulation in patients with complex regional pain syndrome. *Journal of neurology*, *253*(6), 772–9. doi:10.1007/s00415-006-0117-z
Malinen, S., Vartiainen, N., Hlushchuk, Y., Koskinen, M., Ramkumar, P., Forss, N., Kalso, E., et al. (2010). Aberrant temporal and spatial brain activity during rest in patients with chronic pain. *Proceedings of the National Academy of Sciences of the United States of America*, *107*(14), 6493–7. doi:10.1073/pnas.1001504107
Marinus, J., Moseley, G. L., Birklein, F., Baron, R., Maihofner, C., Kingery, W. S., & Van Hilten, J. J. (2011). Clinical features and pathophysiology of complex regional pain syndrome. *Lancet neurology*, *10*(7), 637–648. doi:10.1016/S1474-4422(11)70106-5
McKeown, M J, Makeig, S., Brown, G. G., Jung, T. P., Kindermann, S. S., Bell, a J., & Sejnowski, T. J. (1998). Analysis of fMRI data by blind separation into independent spatial components. *Human brain mapping*, *6*(3), 160–88. Retrieved from http://www.ncbi.nlm.nih.gov/pubmed/9673671
McKeown, Martin J., & Sejnowski, T. J. (1998). Independent component analysis of fMRI data: Examining the assumptions. *Human Brain Mapping*, *6*(5-6), 368–372. doi:10.1002/(SICI)1097-0193(1998)6:5/6<368::AID-HBM7>3.0.CO;2-E
Mori, S., Wakana, S., & Van Zijl, P. (2005). *Atlas of Human White Matter*. Amsterdam, the Netherlands: Elsevier.
Mukherjee, P., Berman, J. I., Chung, S. W., Hess, C. P., & Henry, R. G. (2008). Diffusion tensor MR imaging and fiber tractography: theoretic underpinnings. *American journal of neuroradiology*, *29*(4), 632–41. doi:10.3174/ajnr.A1051
Patterson, R. W., Li, Z., Smith, B. P., Smith, T. L., & Koman, L. A. (2011). Complex regional pain syndrome of the upper extremity. *The Journal of hand surgery*, *36*(9), 1553–62. doi:10.1016/j.jhsa.2011.06.027
Peltz, E., Seifert, F., DeCol, R., Dörfler, A., Schwab, S., & Maihöfner, C. (2011). Functional connectivity of the human insular cortex during noxious and innocuous thermal stimulation. *NeuroImage*, *54*(2), 1324–35. doi:10.1016/j.neuroimage.2010.09.012
Peyron, R., Laurent, B., & García-Larrea, L. (2000). Functional imaging of brain responses to pain. A review and meta-analysis (2000). *Clinical neurophysiology*, *30*(5), 263–88. Retrieved from http://www.ncbi.nlm.nih.gov/pubmed/11126640
Rueckert, D., Sonoda, L., Hayes, C., Hill, D., Leach, M., & Hawkes, D. (1999). Non-rigid registration using free-form deformations: Application to breast MR images. *IEEE transactions on medical imaging*, *18*(8), 712–721.

Schweinhardt, P., & Bushnell, M. C. (2010). Pain imaging in health and disease — how far have we come ? *The Journal of clinical investigation*, *120*(11), 3788–3797. doi:10.1172/JCI43498.3788

Smith, S. (2002). Fast robust automated brain extraction. *Human brain mapping*, *17*(3), 143–155.

Smith, S., Jenkinson, M., Johansen-Berg, H., Rueckert, D., Nichols, T., Mackay, C., Watkins, K., et al. (2006). Tract-based spatial statistics: Voxelwise analysis of multi-subject diffusion data. *NeuroImage*, *31*, 1487–1505.

Smith, S., Jenkinson, M., Woolrich, M., Beckmann, C., Behrens, T., Johansen-Berg, H., Bannister, P., et al. (2004). Advances in functional and structural MRI image analysis and implementation as FSL. *NeuroImage*, *23*(1), 208–219.

Stejskal, E. O., & Tanner, J. E. (1965). Spin diffusion measurements: Spin echoes in the presence of a time-dependent field gradient. *Journal of Chemical Physics*, *42*(1), 288–292.

Swart, C. M. A., Stins, J. F., & Beek, P. J. (2009). Cortical changes in complex regional pain syndrome (CRPS). *European journal of pain*, *13*(9), 902–907. doi:10.1016/j.ejpain.2008.11.010

Tagliazucchi, E., Balenzuela, P., Fraiman, D., & Chialvo, D. R. (2010). *Brain resting state is disrupted in chronic back pain patients. Neuroscience letters* (Vol. 485, pp. 26–31). doi:10.1016/j.neulet.2010.08.053

Van Dijk, K. R. A., Hedden, T., Venkataraman, A., Evans, K. C., Lazar, S. W., & Buckner, R. L. (2010). Intrinsic functional connectivity as a tool for human connectomics: theory, properties, and optimization. *Journal of neurophysiology*, *103*(1), 297–321. doi:10.1152/jn.00783.2009

Woolrich, M., Jbabdi, S., Patenaude, B., Chappell, M., Makni, S., Behrens, T., Beckmann, C., et al. (2009). Bayesian analysis of neuroimaging data in FSL. *NeuroImage*, *45*, S173–186.